

Two-Dimensional Numerical Simulation of Bottom-Gate and Dual-Gate Amorphous In-Ga-Zn-O MESFETs

Chumin Zhao, Linsen Bie, Rui Zhang, and Jerzy Kanicki, *Senior Member, IEEE*

Abstract—In this letter, the electrical properties of bottom-gate and dual gate (DG) amorphous In-Ga-Zn-O (a-IGZO) metal-semiconductor field-effect transistors (MESFETs) are studied by a 2-D numerical simulation. A subgap density of state model is proposed and used in the simulation. The bottom gate MESFET shows field-effect mobility (μ_{FE}) of $9 \text{ cm}^2/\text{V s}$, threshold voltage (V_{th}) of -6.3 V, and subthreshold swing of 0.12 V/decade. The DG a-IGZO MESFET structure is suggested to effectively increase the device operational current (I_{on}).

Index Terms—Amorphous In-Ga-Zn-O (a-IGZO), dual-gate (DG), metal-semiconductor field-effect transistor (MESFET), schottky contact.

I. INTRODUCTION

AMORPHOUS In-Ga-Zn-O (a-IGZO) thin film transistors (TFTs) have attracted much attention and been considered as the next generation TFT technology, due to their high field-effect mobility, low off-current, small subthreshold swing and low fabrication temperature [1]. To improve the TFT electrical performance, the dual-gate (DG) a-IGZO TFT has been proposed and fabricated; a high I_{on} and a steep subthreshold swing without increasing the threshold voltage can be achieved [2]. Most of the TFTs fabricated today require a high-quality gate insulating layer, which still represents a processing challenge for a-IGZO TFTs. The metal-semiconductor field-effect transistors (MESFETs) based on a gate Schottky contact without using a gate insulating layer could simplify device fabrication process. Today research on MESFETs is very limited [3].

In this letter, we present the two-dimensional (2D) numerical simulation as an efficient tool to study the physics of the a-IGZO MESFETs and analyze their electrical properties. We have previously reported a density of states (DOS) model for a-IGZO TFT, which mainly takes into account the DOS adjacent to the conduction band edge [4]. However, for modeling of a-IGZO MESFETs, deep trap states require to be carefully modeled since no charge accumulation occurs and the a-IGZO Fermi-level is located deeper inside the bandgap. Furthermore, to solve the issue of limited free electron concentration in the a-IGZO MESFET channel, the dual-gate MESFET is proposed and simulated, and as expected demonstrates a significant increase of the device operating current.

Manuscript received September 23, 2013; revised October 17, 2013; accepted October 27, 2013. Date of publication November 22, 2013; date of current version December 20, 2013. The review of this letter was arranged by Editor W. S. Wong.

The authors are with the Solid-State Electronics Laboratory, Department of Electrical Engineering and Computer Science, University of Michigan, Ann Arbor, MI 48109 USA (e-mail: kanicki@eeecs.umich.edu).

Digital Object Identifier 10.1109/LED.2013.2289861

TABLE I
KEY A-IGZO PARAMETERS OF SIMULATION AND DEVICE DIMENSION

Symbol	Value	Description / origin
E_g	3.37 eV	Bandgap of a-IGZO / exp.
χ	4.16 eV	Electron affinity / [4]
μ_n	$13.2 \text{ cm}^2(\text{Vs})^{-1}$	Electron band mobility / [4]
N_c	$5 \times 10^{18} \text{ cm}^{-3}$	Effective conduction band DOS / [4]
N_v	$5 \times 10^{18} \text{ cm}^{-3}$	Effective valence band DOS / [4]
N_{ta}	$4.2 \times 10^{19} \text{ cm}^{-3}\text{eV}^{-1}$	Density of conduction band edge states / exp.
N_{td}	$1.5 \times 10^{20} \text{ cm}^{-3}\text{eV}^{-1}$	Density of valence band edge states / [4]
E_a	11 meV	Slope of conduction band tail states / exp.
E_d	110 meV	Slope of valence band tail states / [4]
N_{ga}	$1 \times 10^{17} \text{ cm}^{-3}\text{eV}^{-1}$	DOS peak of acc.-like Gaussian states
N_{gd}	$2 \times 10^{17} \text{ cm}^{-3}\text{eV}^{-1}$	DOS peak of donor-like Gaussian states
λ_a	2.42 eV	Mean energy of acc. Gaussian states / exp.
λ_d	1.0 eV	Mean energy of don. Gaussian states / exp.
σ_a	0.69 eV	Standard deviation (SD) of acceptor-like Gaussian states / exp.
σ_d	0.1 eV	SD of donor-like Gaussian states / exp.
N_{bg}	$2.5 \times 10^{17} \text{ cm}^{-3}$	Background carrier concentration / [3]
W	30 μm	Width
L	5 μm	Gate length
h_{BG}	200 nm	a-IGZO film thickness of BG MESFET
h_{DG}	400 nm	a-IGZO film thickness of DG MESFET
L_{SG}, L_{GD}	2 μm	Gap between S/G and G/D

II. 2D NUMERICAL SIMULATION

A bottom-gate a-IGZO MESFET structure is first employed in the simulation. A high work function gate metal $\phi_M = 5.06\text{eV}$ (Pt) is used to form a Schottky contact. Molybdenum ($\phi_M = 4.33\text{eV}$) is used as the source and drain contact. The Schottky barrier height ϕ_{Bn} is determined by the difference between the metal work function and the electron affinity of a-IGZO (4.16eV): $\phi_{Bn} = \phi_M - \chi = 0.9\text{eV}$. The parabolic field emission model for the gate Schottky contact is used in the simulation [5]. The Schottky barrier height limits the gate voltage to values less than 0.9V, which requires for device to operate within the negative gate voltage range. A thick a-IGZO layer (200nm) is required to achieve a proper full depletion device operation. For dual-gate a-IGZO MESFET simulation, a top-gate with the same dimension is added on top of the a-IGZO layer. Since the depletion region of the top-gate will overlap with the channel opening of the bottom-gate, we have to double the thickness of a-IGZO layer to 400nm. The detailed device dimensions and parameters are shown in TABLE I.

Unlike crystalline materials such as silicon, the bandgap of a-IGZO is filled with trap states that can be described by DOS, which will influence the device performance. Both the

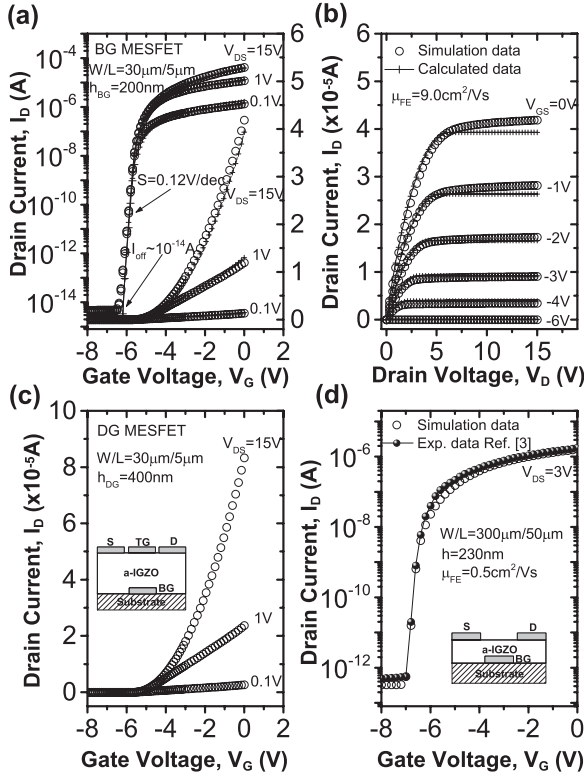


Fig. 1. Simulated transfer characteristics and output characteristics of the bottom-gate a-IGZO MESFET (a, b) and the dual-gate MESFET (c). The calculated data (symbol: +) using standard equations are also shown. Reported experimental results [3] are compared with the simulation data in (d).

subgap band-tail states and the Gaussian distributed gap states are considered in Fig. 3(a). The donor-like states and acceptor-like states are represented as a function of energy (E)

$$g_d = N_{td} \exp[(E_V - E)/kE_d] + N_{gd} \exp[-(E - \lambda_d)^2/\sigma_d^2] \quad (1)$$

$$g_a = N_{ta} \exp[(E - E_C)/kE_a] + N_{ga} \exp[-(E - \lambda_a)^2/\sigma_a^2] \quad (2)$$

where g_d and g_a are the donor-like and acceptor-like states, respectively. The parameters of the exponential donor-like and acceptor-like band tail states were extracted from previous study [4], while the position (λ_d , λ_a) and deviation (σ_d , σ_a) of donor-like and acceptor-like Gaussian states are determined experimentally from combination of optical and electrical measurements. The deep donor-like Gaussian states ($\lambda_d \sim 1.0\text{eV}$) of oxide semiconductors are considered as oxygen vacancy (V_O) states, which are stable when neutral (filled with electrons). The acceptor-like states are found to be responsible for the MESFET threshold voltage shift.

Our study has shown that a background carrier concentration of $N_{bg} \sim 2.5 \times 10^{17} \text{ cm}^{-3}$ is necessary, as an effective n-type doping, to provide the free carriers in the channel. First, the background charge may be induced by the unbalanced ionic charge of the four elements. Second, a-IGZO can be n-type doped by hydrogen or aluminum [6]. Third, the oxygen vacancy states can be ionized and give out two electrons to the conduction band.

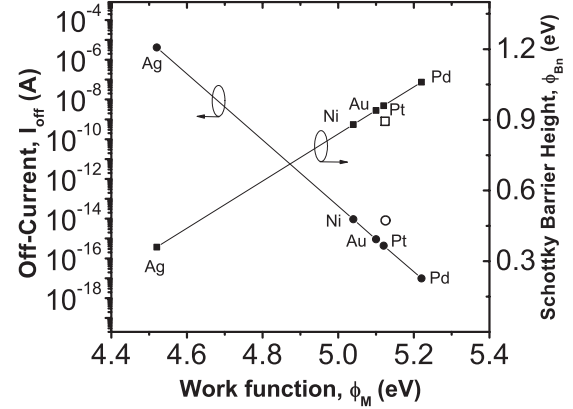


Fig. 2. Simulated off-current (I_{off}) and Schottky barrier height (ϕ_{Bn}) variation with the different gate metal work functions. The experimental data (□, ○) are also shown for Pt Schottky contact.

III. RESULTS AND DISCUSSION

The simulated transfer and output characteristics of the BG and DG MESFETs are shown in Fig. 1(a-c). The BG MESFET shows field-effect mobility of $9.0 \text{ cm}^2/\text{Vs}$, threshold voltage of -6.3 V , subthreshold swing of 0.12 V/dec and off-current smaller than 10^{-14} A . The simulated data fit the standard equations well [7], which indicates the simulation model is reliable. The channel width/length (W/L) in the simulation is $30 \mu\text{m}/5 \mu\text{m}$; W/L does not affect mobility. However, W/L and the source/gate (gate/drain) separation will influence the device operational current and needs to be optimized.

The simulation result shows that the off-current exponentially decays with the increasing of the gate metal work function or barrier height (Fig. 2) with no changes of other device parameters such as the mobility, threshold voltage and sub-threshold swing. The off-current is dominated by the gate leakage current flowing from the drain to the gate and is well described by reverse-biased Schottky junction equation [7]. Since off-current is inversely exponentially proportional to Schottky barrier height, metals with a high work function such as Pt and Pd must be used as the gate to achieve $\phi_{Bn} \sim 1 \text{ eV}$ and a low off-current ($< 10^{-14} \text{ A}$). The experimental Schottky barrier height of Pt and corresponding off-current [3] are also shown in Fig. 2. The off-current of fabricated device has been normalized to designed device dimension used in simulation. To achieve sufficiently high barrier height and low off-current, low density of defects at the metal-semiconductor interface is essential.

The threshold voltage (V_{th}) of MESFET devices is determined by $V_{th} = V_{bi} - V_P$. The built-in potential (V_{bi}) and the pinch-off voltage (V_P) are given by

$$V_{bi} = \phi_{Bn} - (kT/q) \ln(N_C/n) \quad (3)$$

$$V_P = q(N_{bg} - N_A^-)h^2/2\varepsilon_S \quad (4)$$

where n is the channel free carrier density, N_{bg} is the background carrier concentration (cm^{-3}) and N_A^- is the depletion region concentration of ionized acceptor-like states (cm^{-3}). The calculated V_{bi} and V_P are 0.8V and 7.1V , respectively;

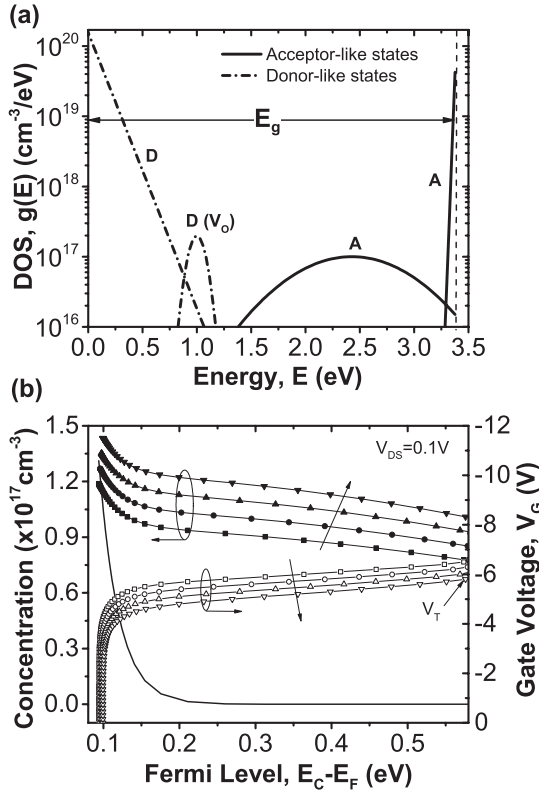


Fig. 3. (a) a-IGZO density of states (DOS) model used in the simulation. (b) Simulated ionized acceptor-like states concentration (N_A , solid symbol), free electron concentration (n , —) and gate voltage (V_G , open symbol) of the bottom-gate a-IGZO MESFET as a function of the Fermi-level position. Impact of various DOS peak of acceptor-like Gaussian states (N_{ga}) is investigated; data for N_{ga} of 1.0 (■, □), 1.1 (●, ○), 1.2 (▲, △) and $1.3 \times 10^{17} \text{ cm}^{-3} \text{ eV}^{-1}$ (▼, ▽) are shown.

which gives the threshold voltage $V_T = -6.3\text{V}$. Both simulation and calculation demonstrate that a thicker a-IGZO layer shifts the threshold voltage to more negative values, thus broadens the device operation region. N_{bg} and N_A^- are found to be responsible for the threshold voltage value. Fig. 3(b) shows the simulated ionized acceptor-like states concentration, free electron concentration and gate voltage of the bottom-gate a-IGZO MESFET as a function of the Fermi-level position. The probe position is inside the channel opening, close to the top surface. As the result of raising the DOS peak of the acceptor-like Gaussian states (N_{ga}), the ionized acceptor-like states concentration increase, which leads to a positive threshold voltage shift. In addition, for a given energy position, a large value of N_{ga} will lead to a poor subthreshold slope. The energy level of the acceptor-like states also influences the threshold voltage. Deeper energy level leads to a more positive threshold voltage due to the larger value of N_A^- in Eq. (4). It should be noticed that the Fermi-level position has to be elevated to $E_C - E_F < 0.3 \text{ eV}$ to gain enough free electrons

and make the MESFET work. Therefore, a sufficiently large background carrier concentration $\sim 2.5 \times 10^{17} \text{ cm}^{-3}$ is required.

Without increasing the dimension of the device, the BG a-IGZO MEFEST could be modified to DG a-IGZO MESFET by doubling the a-IGZO film thickness. This approach will allow to double the device operational current without any additional changes. The DG MESFET schematics and corresponding transfer characteristics are shown in Fig. 1(c).

To our best knowledge, only one experimental data on a-IGZO MESFETs was reported [3], which provides a low field-effect mobility (μ_{FE}) of $0.5 \text{ cm}^2/\text{Vs}$. To calibrate the simulation model, the experimental data is extracted and compared with our simulated result in Fig. 1(d). To fit the experimental results, we had to only reduce the a-IGZO electron band mobility (μ_n) to $0.9 \text{ cm}^2/\text{Vs}$. Very good fit between simulated and experimental data validates the simulation model.

We believe that a-IGZO MESFET is a possible candidate for liquid crystal display as the switching transistor in the future.

IV. CONCLUSION

We have developed the DOS model for a-IGZO MESFET simulation. Both the BG and DG a-IGZO MESFETs have been simulated, and their electrical characteristics have been investigated. High Schottky barrier height is critical to achieve a low off-current. The background charge density and the acceptor-like states density are critical for the threshold voltage control. To solve the problem of the limited free carrier and to increase the device on-current, the DG a-IGZO MESFET is proposed.

REFERENCES

- [1] K. Nomura, H. Ohta, A. Takagi, *et al.*, "Room-temperature fabrication of transparent flexible thin-film transistors using amorphous oxide semiconductors," *Nature*, vol. 432, no. 7016, pp. 488-492, Nov. 2004.
- [2] G. Baek, K. Abe, A. Kuo, *et al.*, "Electrical properties and stability of dual-gate coplanar homojunction DC sputtered amorphous indium-gallium-zinc-oxide thin-film transistors and its application to AM-OLEDs," *IEEE Trans. Electr. Device*, vol. 58, no. 12, pp. 4344-4353, Dec. 2011.
- [3] D. H. Lee, K. Nomura, T. Kamiya, *et al.*, "Metal-semiconductor field-effect transistor made using amorphous In-Ga-Zn-O channel and bottom Pt Schottky contact structure at 200 °C," *ECS Solid State Lett.*, vol. 1, no. 1, pp. 8–10, Jul. 2012.
- [4] T.-C. Fung, C.-H. Chuang, C. Chen, *et al.*, "Two-dimensional numerical simulation of radio frequency sputter amorphous In-Ga-Zn-O thin-film transistors," *J. Appl. Phys.*, vol. 106, no. 8, pp. 084511-1–084511-10, Oct. 2009.
- [5] *ATLAS Device Simulation Software User's Manual*, Silvaco International, Santa Clara, CA, USA, Dec. 2005.
- [6] T. Kamiya, K. Nomura, and H. Hosono, "Origins of high mobility and low operation voltage of amorphous oxide TFTs: Electronic structure, electron transport, defects and doping," *J. Display Technol.*, vol. 5, no. 7, pp. 273–288, Jul. 2009.
- [7] S. M. Sze and K. K. Ng, "JFETs, MESFETs and MODFETs," in *Physics of Semiconductor Devices*, 3rd ed. New York, NY, USA: Wiley, 2007, pp. 374–400, Ch. 7.